Modulation of H+/H- Exchange within Iridium-hydride 2-Hydroxypyridine Complexes by Remote Lewis Acids

SCHOLARONE™
Manuscripts

Journal Name

COMMUNICATION

Modulation of H+/H- Exchange of Iridium-hydride 2-Hydroxypyridine Complexes by Remote Lewis Acids†

J. P. Shanahan,[a] C. M. Moore,[b] Jeff W. Kampf[c] and N. K. Szymczak*[c]

A series of iridium hydride complexes featuring dihydrogen bonding are presented and shown to undergo rapid H+/H- exchange (1240 s^{-1} at 25 °C). We demonstrate that the H+/H- exchange rate can be modified by post-synthetic modification at a remote site using BH$_3$, Zn(C$_6$F$_5$)$_2$, and Me$_3$O[BF$_4$]. This route provides a complementary strategy to traditional methods that rely on pre-metalation modifications to a metal's primary sphere.

The heterolytic activation of dihydrogen is central to both biological and abiological energy conversion/storage schemes.[1] Hydrogenase enzymes exploit extremely rapid and reversible proton/hydride interconversions for energy storage and release.[2] [Fe]-hydrogenase contains a biologically unusual 2-hydroxypyridine motif and this bifunctional ligand has been proposed to serve a unique role; facilitating reversible H$_2$ heterolysis into hydride and proton equivalents (Figure 1A).[3] Our group[4] and others[5] have shown that synthetic complexes featuring 2-hydroxypyridine derived ligands can mediate H+/H- exchange[4c] and promote reversible hydrogenation/dehydrogenation reactions.[5a, 6] Computational studies of [Fe]-hydrogenase have shown that the rate of H$_2$ activation is tunable, and intimately tied to the electronic environment at the iron center, as modulated by subtle perturbations to both the primary and secondary coordination environment.[7]

Assessing the interplay between primary-sphere modifications and secondary-sphere effects that control the reactivity of [Fe]-hydrogenase (and inspired synthetic systems) can provide new design principles to improve activity for

hydrogenative or dehydrogenative reactivity.[8] In analogy to [Fe]-hydrogenase, iridium (III) hydride complexes have low spin d^6 electronic configurations and increased stability.[9] Thus, iridium complexes can be used to assess the extent to which a given H$_2$ transformation may be regulated by subtle changes to the metal electronic environment and/or appended acidic groups.[10]
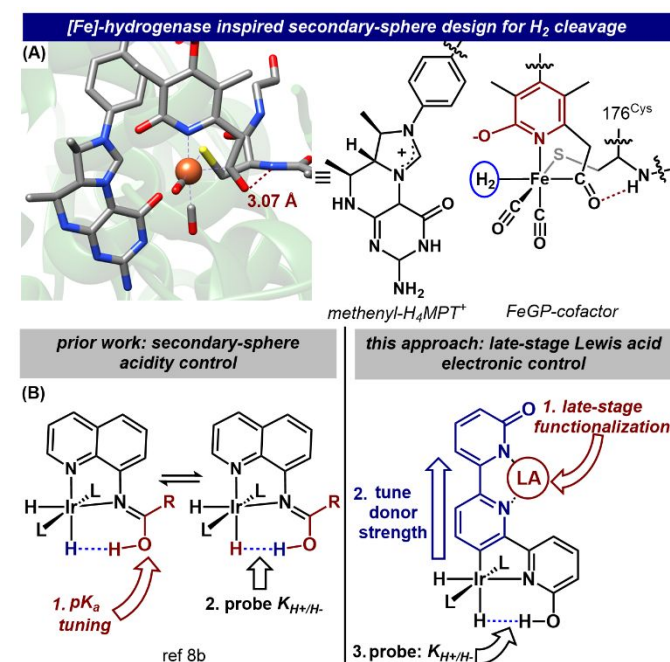

Figure 1. Dihydrogen bond motifs in (A) [Fe]-hydrogenase (Protein Databank: 6hae) and (B) synthetic complexes with pK_a (left) and remote modification control (right).

Transition-metal hydrides engaged in dihydrogen-bonding have been proposed to be key intermediates in heterolytic H$_2$ activation (Figure 1B). Their key reactions, which include H+/H- exchange and (de)hydrogenation catalysis, are sensitive to the supporting ligands (electronic donation[10a] steric hindrance,[10b] and metal cation induced hemilability).[7, 11,12] Most prior examples to tune the H$_2$ heterolysis rate have been through

a Department of Chemistry, Columbia University, New York, New York 10027, USA.
b Chemistry Division, Los Alamos National Laboratory, MS K558, Los Alamos NM 87545, USA.
c Department of Chemistry, University of Michigan, 930 N. University Ave., Ann Arbor, MI 48109-1055, USA. E-mail: nszym@umich.edu

modifications to the metal's primary coordination sphere.[8c] As an alternative to inner-sphere electronic modifications, strategies
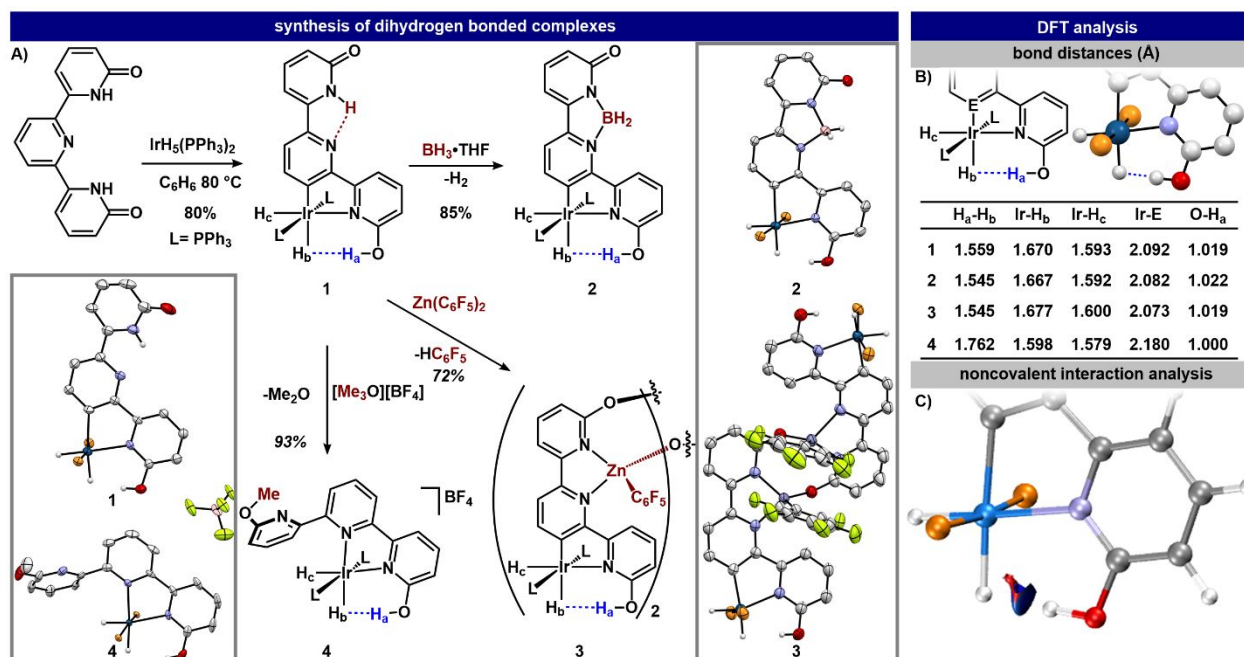

Figure 2. (A) Synthesis and crystal structure of **1**, **2**, **3**, and **4**. Ellipsoids are shown at the 50% probability level and hydrogen atoms bound to carbon, phenyl rings and the BF_4^- anion of **4** are removed for clarity . (B) Calculated primary and secondary-sphere bond distances with representative structure of **1**. (C) Representative dihydrogen bond critical point of **1**.

that functionalize ligands at remote sites have been shown to regulate metal centered electronic properties, and impart large changes to reaction rates[13] and selectivity.[14] To extend this concept, we demonstrate how H^+/H^- exchange rates of dihydrogen bonded iridium hydrides vary as a function of remote functionalization.

To interrogate the extent to which an H_2 heterolysis rate can be tuned by modifications at a remote ligand site, we prepared a series of dihydrogen bonded iridium hydrides. The metalation of 6,6'-dihydroxyterpyridine (dhtp) with $Ir(H)_5(PPh_3)_2$ afforded the rollover C-H activated terpyridine complex $Ir(H)_2(dhtp')(PPh_3)_2$ (**1**) (Figure 2A). Crystallographic analysis indicated that one of the two 2-hydroxypyridine units was not coordinated to iridium and remained in the 2-pyridone tautomeric form. Although the X-ray structure indicated two Ir-H environments, the ^{1}H NMR spectrum at ambient temperature exhibited only one triplet resonance at high field (-17.59 ppm; $^2J_{HP}$ = 16.5 Hz) as well as one low field −*NH* resonance at 10.55 ppm. Upon cooling, two additional broad peaks were resolved: a resonance at 9.94 ppm and a second low field resonance (-11.45 ppm) assigned as H_a and H_b respectively (Figure 2). Analysis of the spin-lattice relaxation times, T_1, of H_a and H_b revealed short (0.18(1) s; 248 to 258 K, 500 MHz), and equivalent values at all measured temperatures, consistent with a dynamic exchange process.

To evaluate how the dihydrogen bonding interaction from the 2-hydroxypyridine group influences the structural dynamics and reactivity of the iridium hydrides, we investigated the H^+/H^- exchange behavior of **1**. Upon addition of 1000 equivalents

CD_3OD to **1**, the NH, H_a, and H_b ^{1}H NMR resonances diminished within 5 minutes. The results are consistent with H/D exchange with the NH and H_a followed by a subsequent D^+/H^- exchange between H_a and H_b. In contrast, no deuterium incorporation at the H_c position was observed after 2 days; inconsistent with dynamic exchange of H_c.[15]

We hypothesized that the interaction between H_a and H_b could be perturbed by altering the electronics at Ir. In addition to a κ-C,N dhtp' primary coordination environment, **1** also features a remote bipyridine-like site (Figure 1B). To modulate H^+/H^- exchange rates, we targeted remote functionalization of the bipyridine-like fragment. We envisioned that induction through the pyridone *para* to the Ir-C bond would strongly perturb donor properties, and thus, the basicity of the iridium hydride, H_b. Two Lewis acids were incorporated into the bipyridine-like site. The reaction of **1** with either $NaBH_4$ or $THF•BH_3$ afforded $Ir(H)_2(dhtp-BH_2)(PPh_3)_2$ (**2**) (Figure 2A), which was characterized by X-ray crystallography. Addition of $Zn(C_6F_5)_2$ to **1** afforded the dimeric compound $[Ir(H)_2(dhtp-Zn(C_6F_5))(PPh_3)_2]_2$ (**3**) (Figure 2) with loss of C_6F_5H (Figure S35). Analysis of the $^{31}P\{^1H\}$ spectrum of **3** revealed two signals, consistent with a dimeric structure in solution.[16] To maximize the electron withdrawing ability of the remote functionalization partner, we targeted an alkylation (CH_3^+) strategy to impart a coulombic charge difference on the ligand. Selective methylation of **1** was achieved using $[Me_3O]BF_4$ to generate $Ir(H)_2(tpy^{OHOMe}- \kappa^2-N,N)(PPh_3)_2BF_4$ (**4**) in good yield (93 %; Figure 2). Importantly, alkylation of the dhtp ligand afforded a primary sphere rearrangement from κ^2-C,N to κ^2-N,N coordination.

Journal Name　　　　　　　　　　　　　　　　　　　　　　　　　　　　**COMMUNICATION**

The late-stage functionalized complexes were characterized by NMR spectroscopy to assess dynamic H^+/H^- exchange processes. Both **2** and **3** exhibited similar ^{1}H NMR spectra to **1** at high field: one triplet was observed at room temperature and a second broad singlet appeared upon cooling. For both **2** and **3**, a single low field resonance appeared upon cooling (10.41 ppm and 9.80 ppm respectively), consistent with only small changes to the pendent hydroxyl group acidity, compared to **1.** In contrast to **1-3**, the cationic complex **4** exhibited two triplet of doublet high field resonances (-17.66 ppm and -20.27 ppm) at room temperature, each coupling to both each other $^2J(H_b$-$H_c)$ 8 Hz, and to the PPh$_3$ ligands. The high field resonance at -20.16 ppm was identified as H_b by a 1D NOESY detected close contact to H_a; representing an 8.7 ppm shift from **1** upon changing the *trans*-donor ligand.

Since crystallographic determination of H_a-H_b distances are often imprecise, we calculated the H-H distance using the dipolar relaxation contribution to the T_1(min) value.[17] For complexes **1-3**, the T_1 (min) for the H_a and H_b were equivalent and span 0.172 (2) s at 238 K (**2**) to 0.247 (11) at 268 K (**3**) (Figure S4). In contrast, the T_1 values for H_a and H_b of **4** were *inequivalent* (T_1 (min) H_a = 0.369(10) s at 253 K; H_b = 0.200(13) s at 273 K). The corresponding H_a-H_b distances of **1**, **2**, and **4** were calculated[17] to be between 1.8-2.0 Å (Table S8), indicating similar local primary (Ir-(H)$_2$) and secondary sphere 2-hydroxypyridine geometries (See SI for full discussion). We attribute the similar distances for the series to the rigid coordination geometry at Ir imposed by the dhtp ligand scaffold.[18]

Compounds **1**-**3** feature distinct electronic environments at Ir, via remote modification, and thus provide a unique opportunity to examine differences in dihydrogen bonding interactions and H^+/H^- exchange. The short H-H contacts are consistent with a dihydrogen bond interaction and were further supported by detection of through-space ^1J coupling through the dihydrogen bond at low temperatures (Figure S2). The low field resonances of **1**, **2**, and **3** featured $^1J_{HH}$ coupling with values of 6.9 Hz, 8.7 Hz and 6.5 Hz at 238 K respectively. The smaller $^1J_{HH}$ for **2** and **3** and absence of observable coupling for **4** are consistent with weaker dihydrogen bonding interactions than in **1**, imparted by perturbing the *trans*–C ligand donor, and thus Ir-H strength. Combined, the ^{1}H NMR analyses (*vide infra*) provide multiple sets of data that enable the dihydrogen bond interaction to be scrutinized. Data for compounds **1**, **2**, and **3** are consistent with rapid exchange between the H_a and H_b positions. However, the spectral data for **4** (inequivalent T_1 values and no $^1J(H_a$-$H_b)$ coupling) are consistent with a static structure at room and low temperature, despite the close contact analogous to **1-3**.[19] To evaluate the perturbations of H^+/H^- exchange upon remote functionalization, we determined the exchange rates and associated thermodynamic parameters for compounds **1-3**. The rate of H_a/H_b exchange was determined by a variable temperature ^{1}H NMR spin-saturation transfer, where irradiation of H_b caused a loss of signal intensity of H_a.[20] The extrapolated room temperature $\Delta G^\ddagger$ and exchange rates (rate$_{298K}$) were determined through an Eyring analysis (Table 1). For –H, –BH$_2$, –ZnL$_2$, the rate$_{298K}$ are 1240 s^{-1}, 350 s^{-1}, and 390 s$^-$

[1], respectively. A maximum limit for the exchange rate of **4** at 298 K was calculated to be 0.42 s^{-1}.[21] In contrast, complexes **1-3** exhibit the fastest exchange rate among reported Ir-dihydrogen bonds; outcompeting the rate$_{298K}$ = 62.8 s^{-1} for the most acidic iminol quinoline complex.[8b22]

Table 1. Experimental $\Delta G^\ddagger_{298K}$, extrapolated rate of H^+/H^- exchange, H-bond strength (E_{HB}) and NBO charge at Ir of **1-4**.

	$\Delta G^\ddagger_{298K}$ (kcal/mol)	Rate$_{298K}$ (s^{-1})	E_{HB} (kcal/mol)	Ir NBO Charge
1	13.2 (2)	1240 ± 430	-7.2	-1.22
2	14.0(2)	350 ± 120	-7.8	-1.21
3	13.9(2)	390 ± 134	-7.5	-1.23
4	-	< 0.42	-5.1	-1.01

The likely mechanism for H^+/H^- exchange proceeds via deprotonation of the pendent hydroxyl group to afford an intermediate η^2-H_2 complex, which upon rotation is subsequently deprotonated by the pendent 2-pyridone base.[2324] The barrier for the rotation of η^2-H_2 in metal-dihydrogen complexes is generally small (< 3 kcal/mol), relative to proton transfer.[25] Since exchange facilitated by a rigid bidentate ligand requires minimal reorganization energy, the rate of exchange is proposed to be limited by pK_a matching of the η^2-H_2 intermediate and the pendent hydroxyl group. The late-stage functionalization imparts increasing hydricity of H_b across the series - κ^2-*N,N* (CH$_3^+$) < –BH$_2^+$≈ –ZnL$_2$ < –H$^+$ and thus, increasing basicity, favoring deprotonation of the pendent hydroxyl group. For **4**, we propose that the lack of H^+/H^- exchange is due to both the decreased hydricity of H_b (containing a weaker *trans-N* donor), and the cationic charge of the complex. Alternatively, ion pairing effects with the BF$_4^-$ anion in **4** could inhibit intramolecular exchange.[10b2616,36]

To interrogate the impact that ligand functionalization imparts on the electronic structure of **1-4**, we used computational methods. Structure optimization, charge, and bonding analysis were calculated using methods that are highly reliable for both iridium transformations,[27] and H-bonding.[28, 29] To assess the electronic effects from remote functionalization, we evaluated the NBO charges, and found that the perturbations at Ir and H_b track with the exchange behavior of **1-4** (Table 1). Structural analysis of the primary sphere (Figure 2B, Tables S7 and S9) feature Ir-H_b distances that report on the electronic differences of the *trans-* donor ligand: - κ^2-*N,N* (CH$_3^+$) << –BH$_2^+$ ≈ –ZnL$_2$ < –H$^+$, and identical to the observed exchange rates. A *trans-* donor controlled rather than secondary-sphere pK_a controlled exchange is further supported by minimal changes to the calculated H-bond donor proton (H_a) charge for **1-4**. The computational analyses demonstrate that ligand tuning effects of Lewis acids can serve as an important role to effect secondary-sphere facilitated reactions.

To assess how the ligand perturbations influence the H-bond interaction, we analyzed bond critical points[30] along the dihydrogen bond H_a-H_b coordinate (Figure 2C). From the calculated potential energy density at the critical point ($V(r_{BCP})$), we found that the H-bond energies (E_{HB})[31] spanned -7.8 to -5.1 kcal/mol (**2** and **4** respectively). Although the energies for **1-3** (< 1 kcal/mol) did not track with the observed exchange rates, the differences were small and we attribute these to a combination

of the small geometric differences of the Ir-E distances, as well as small electronic changes of the optimized complexes. For instance, compound **2** was optimized to have a slightly shorter Ir–C contact (ΔIr–C = 0.009 Å) than **1**, which repositions the chelating 2-hydroxypyridine ligand fragment for a closer H-bond contact (ΔH_a–H_b = 0.003 Å) and a stronger H-bond interaction. These subtle changes in H-bond energies for **1**-**3** emphasize that discrete remote functionalization from electronic effects can be minor[32] and, in this case, competitive with small geometric changes to the molecules.

In summary, we showed that late stage functionalization of **1** can impart: (1) control of H^+/H^- exchange rate by 1000 s^{-1} and (2) influence the ΔG of proton transfer. The 2-hydroxypyridine ligand exerts an unusually strong dihydrogen bond with the iridium hydrides that influence H_2 heterolysis. Rapid equilibria established for the iridium systems **1-3** are analogous to the low spin d^6 metal center in [Fe]-hydrogenase. The remote electronic perturbation at the metal center further highlights the sensitivity of H_2 heterolysis mechanisms to the ancillary ligands. This approach could provide future applications for late stage modification of (de)hydrogenation catalysts where hydricity fine-tuning could be used to influence proton reduction vs hydrogen oxidation pathways.[33]

Conflicts of interest

There are no conflicts to declare.

Notes and references

1. (a) T. R. Cook, D. K. Dogutan, S. Y. Reece, Y. Surendranath, T. S. Teets and D. G. Nocera, *Chem. Rev.*, 2010, **110**, 6474-6502; (b) R. M. Bullock and M. L. Helm, *Acc. of Chem. Res.*, 2015, **48**, 2017-2026.
2. W. Lubitz, H. Ogata, O. Ruediger and E. Reijerse, *Chem. Rev.*, 2014, **114**, 4081-4148.
3. (a) C. M. Moore, E. W. Dahl and N. K. Szymczak, *Curr.Opin. Chem. Bio.*, 2015, **25**, 9-17; (b) S. Shima, O. Pilak, S. Vogt, M. Schick, M. S. Stagni, W. Meyer-Klaucke, E. Warkentin, R. K. Thauer and U. Ermler, *Science*, 2008, **321**, 572; (c) G. Huang, T. Wagner, M. D. Wodrich, K. Ataka, E. Bill, U. Ermler, X. Hu and S. Shima, *Nat. Catal.*, 2019, **2**, 537-543.
4. (a) S. Mizuta, I. S. R. Stenhagen, M. O'Duill, J. Wolstenhulme, A. K. Kirjavainen, S. J. Forsback, M. Tredwell, G. Sandford, P. R. Moore, M. Huiban, S. K. Luthra, J. Passchier, O. Solin and V. Gouverneur, *Org. Lett.*, 2013, **15**, 2648-2651; (b) C. M. Moore and N. K. Szymczak, *Chem. Commun.*, 2013, **49**, 400-402; (c) J. B. Geri and N. K. Szymczak, *J. Am. Chem. Soc.*, 2015, **137**, 12808-12814.
5. (a) G. Zeng, S. Sakaki, K.-i. Fujita, H. Sano and R. Yamaguchi, *ACS Catal.*, 2014, **4**, 1010-1020; (b) D. Deng, B. Hu, Z. Zhang, S. Mo, M. Yang and D. Chen, *Organometallics*, 2019, **38**, 2218-2226.
6. C. M. Moore, B. Bark and N. K. Szymczak, *ACS Catal.*, 2016, **6**, 1981-1990.
7. A. R. Finkelmann, M. T. Stiebritz and M. Reiher, *J. Phys. Chem. B*, 2013, **117**, 4806-4817.
8. (a) J. B. Geri, J. L. Ciatti and N. K. Szymczak, *Chem. Commun.*, 2018, **54**, 7790-7793; (b) J. C. Lee, E. Peris, A. L. Rheingold and R. H. Crabtree, *J. Am. Chem. Soc.*, 1994, **116**, 11014-11019; (c) E. S. Wiedner, M. B. Chambers, C. L. Pitman, R. M. Bullock, A, J. M. Miller, and A. M. Appel, *Chem. Rev.* 2016, **116**, 8655-8692.
9. J. F. Hartwig, *Organotransition metal chemistry : from bonding to catalysis*, University Science Books, Sausalito, CA, 2010.
10. (a) S. H. Park, A. J. Lough, G. P. A. Yap and R. H. Morris, *J. Organomet. Chem.*, 2000, **609**, 110-122; (b) K. Gruet, E. Clot, O. Eisenstein, D. H. Lee, B. Patel, A. Macchioni and R. H. Crabtree, *New J. Chem.*, 2003, **27**, 80-87.
11. (a) N. V. Belkova, L. M. Epstein, O. A. Filippov and E. S. Shubina, *Chem. Rev.*, 2016, **116**, 8545-8587; (b) A. J. Lough, S. Park, R. Ramachandran and R. H. Morris, *J. Am. Chem. Soc.*, 1994, **116**, 8356-8357; (c) J. C. Lee, A. L. Rheingold, B. Muller, P. S. Pregosin and R. H. Crabtree, *J. Chem. Soc., Chem. Commun.*, 1994, 1021-1022; (d) E. Peris and R. H. Crabtree, *J. Chem. Soc., Chem. Commun.*, 1995, 2179-2180.
12. M. R. Kita and A. J. M. Miller, *J. Am. Chem. Soc.*, 2014, **136**, 14519-14529.
13. (a) K. T. Horak, D. G. VanderVelde and T. Agapie, *Organometallics*, 2015, **34**, 4753-4765; (b) A. L. Liberman-Martin, R. G. Bergman and T. D. Tilley, *J. Am. Chem. Soc.*, 2013, **135**, 9612-9615.
14. K. N. T. Tseng, J. W. Kampf and N. K. Szymczak, *ACS Catal.*, 2015, **5**, 411-415.
15. Spin saturation transfer NMR experiments confirmed no exchange between H_b and H_c.
16. A persistent side-product was formed in 10-20% as evident by NMR spectroscopy. We assign this compound as the competing diastereomer from dimer formation with Zn-C_6F_5 orrented on opposite faces.
17. P. J. Desrosiers, L. Cai, Z. Lin, R. Richards and J. Halpern, *J. Am. Chem. Soc.*, 1991, **113**, 4173-4184.
18. (a) W. Xu, A. J. Lough and R. H. Morris, *Can. J. Chem.*, 1997, **75**, 475-482; (b) T. B. Richardson, T. F. Koetzle and R. H. Crabtree, *Inorganica Chim. Acta*, 1996, **250**, 69-73.
19. Heating **4** in CDCl$_3$ from 298 K to 328 K, increased the observed 1D NOESY(EXSY) cross peak between H_a and H_b of 4 by 36 %, which indicated slow exchange may occur above ambient temperature.
20. R. L. Jarek, R. J. Flesher and S. K. Shin, *J. Chem. Ed.*, 1997, **74**, 978.
21. This value was obtained using the magnetization transfer rate detemination at 298 K assuming a 5% error for the integration of both M_0 and M_{0a} and using the smaller T_1 for the exchanging resonances to obtain an upper limit on the calculated rate.
22. Extrapolation of the calculated thermodynamic parameters for the iminol quinolone compound ($\Delta G^{\ddagger}$293 K 15 ± 2 kcal/mol quinoline system R= 3,4-$C_6H_4F_2$) in Figure 1b.
23. R. Koelliker and D. Milstein, *J. Am. Chem. Soc.*, 1991, **113**, 8524-8525.
24. Serial dilution of a solution of **1** did not influence on the exchange rate, supporting an intramolecular mechanism. See Figure S6.
25. G. J. Kubas, *Chem. Rev.*, 2007, **107**, 4152-4205.
26. However, the static description of **4** was found to be concentration independent and no tight ion pair could be detected by $^{19}F^1H$ HOESY at maximum concentration.
27. K. H. Hopmann, *Organometallics*, 2016, **35**, 3795-3807.
28. (a) S. Grimme, J. Antony, S. Ehrlich and H. Krieg, *J. Chem. Phys.*, 2010, **132**, (b) S. Grimme, *J. Comput. Chem.*, 2006, **27**, 1787-1799.
29. The calculations of dimer complex **3** have been prohibitively long.
30. R. F. W. Bader, *Acc. of Chem. Res.*, 1985, **18**, 9-15.
31. E. Espinosa, E. Molins and C. Lecomte, *Chem. Phys. Lett.*, 1998, **285**, 170-173.
32. J. P. Shanahan and N. K. Szymczak, *Organometallics*, 2020, **39**, 4297-4306.
33. S. Raugei, M. L. Helm, S. Hammes-Schiffer, A. M. Appel, M. O'Hagan, E. S. Wiedner, R. M. Bullock, *Inorg. Chem.* 2016, **55**, 445-460.